IEEE Transactions on Nuclear Science, Vol. NS-28, No. 6, December 1981

SURFACE FLASHOVER ARC ORIENTATION ON MYLAR FILM*

M. Gossland and K.G. Balmain
Department of Electrical Engineering
University of Toronto
Toronto, Canada M5S 1A4

M.J. Treadaway
JAYCOR
P.O.Box 85154
San Diego, CA 92138

Abstract

A study of the arc discharge patterns and resultant damage patterns on thin Mylar films exposed to a 20 keV electron beam is described. In particular, it is established that there is a broad directional correlation among the directions associated with visible linear arcs, damage tracks, the "slow" optical direction and the longitudinal marks left on the film surface as a result of chemical etching. Transverse etch marks also appear to be associated with secondary groups of damage track directions. The "fast" optical direction is associated with the absence of visible arcs or arc damage.

Introduction

In crystalline insulating materials there exists a tendency for electrical breakdown to occur preferentially along well defined crystallographic directions, a phenomenon first observed over fifty years ago[1]. It is known that Mylar film is partially crystalline[2] and is therefore optically birefringent and anisotropic in some of its physical characteristics[3] (e.g., tensile strength, stiffness, and tear strength). During manufacture, Mylar film is stretched either uniaxially or biaxially, a process which increases its crystallinity[2,4]. Evidence suggests that at least the surface layer of biaxially stretched Mylar is composed of quasi-rectangular crystalline regions surrounded by a network of amorphous material, with the major axis of the rectangles falling along the initial stretch direction[3,5]. This pattern is revealed by a chemical etchant that preferentially attacks the amorphous regions, thereby creating channels between the crystalline blocks and producing a characteristic microscopic "brick and mortar" appearance.

In the course of spacecraft charging simulations, it has been found that electron-beam-charged polymer films sometimes exhibit very regular straight-line surface damage tracks following arc discharges[6,7] and recently Yadlowsky, et al.[8] in studying such damage tracks on Teflon have been able to associate the track directions with (a) elongated regions of surface charge cleanoff, (b) orientation of the specimen edge for minimum breakdown beam energy, and (c) characteristic optical directions of the birefringent material. In this paper electron-beam-charged and multiple-arc-discharged Mylar film will be considered with attention given to the orientations associated with

(a) various types of microscopic damage tracks;

(b) macroscopic discharge arcs photographed with an open shutter technique;

(c) the optical anisotropy of the birefringent material;

(d) the crystalline structure of the material as revealed by chemical etching.

Damage Track Study

Three of the four specimens studied in this work were cut from a meter-diameter sheet of 75 μm aluminized Mylar shown undergoing discharge in Fig.1 which also depicts the specimen locations. The specimens were taken from areas where the vacuum-deposited aluminum backing had been blown off by the discharge so that microscopic observations could be made with reflected or transmitted light without having to remove the metal chemically. Another specimen was obtained from a 30 cm^2 piece of 75 μm unmetallized Mylar which had been irradiated while in contact with a metal backing plate. Because each sample was only a few square centimeters in area it was assumed that the properties measured (to be described) would not vary significantly over each specimen's extent, thus enabling meaningful intra-specimen comparisons of those properties to be made. All specimens had been exposed to a 20 keV electron beam.

The damage tracks were easily seen under the microscope with as little as ×250 magnification (×20 obj., ×12.5 eyepiece) and were immediately categorizable into 4 track types:

(1) long straight tracks up to several cm in length and sometimes occurring in pairs roughly 5 μm apart;

(2) curved tracks usually less than 1 cm in length;

(3) very short (4 μm) leafy projections from types 1 and 2 above, typically branching off at 60°;

(4) longer tracks resembling tree branches with a forking angle of approximately 30°.

In each of the above cases the track depth lies within the top 5 μm, based on a calibration of the microscope focussing adjustment. These damage tracks were photographed through both an optical microscope (OM) and a scanning electron microscope (SEM), and typical examples of the four track types are shown in the OM photograph in Fig.2. On the left is a track of type 2 accompanied by type 3 tracks and on the right is a pair of typically straight type 1 tracks with short type 3 projections and long type 4 projections. An SEM photograph of the same feature at a similar magnification is shown in Fig.3 where the tracks of type 4 appear shallower than the others.

A close-up of the vertex region (Fig.4) suggests that no tracks are deeper than 1 μm while revealing also that each straight track consists of a series of pits. In addition, the leafy projections of type 3 appear to be troughs terminated by pits or sometimes

* Work supported by the U.S. Air Force Weapons Laboratory and by NASA through Grant NSG-7647, and by the Natural Sciences and Engineering Research Council of Canada, through Operating Grant A-4140.

0018-9499/81/1200-4535$00.75©1981 IEEE

nodules. The area in the lower right hand corner was also photographed at a higher magnification (Fig.5).

One more example of damage was photographed through both the OM and the SEM (Figs.6, 7 and 8). Again the branch-like tracks of type 4 appear to be the most superficial. The projections of type 3 seen at a higher magnification in Fig.8 look as if they could be sites where molten beads of plastic were deposited on the surface.

In attempting to associate track appearance with arc propagation direction, one might assume either that the type 4 tracks are created by the discharge starting at the extremes (terminations) and propagating toward the vertices (joints with larger tracks) like the drainage in a river system, or propagating from the vertices toward the extremes like the growth of a tree branch. In either case, the two sets of nearly parallel type 4 tracks shown in Fig.9 suggest opposing directions of propagation. This in turn suggests that the factors governing the propagation direction can vary significantly from one discharge to another.

In spite of this type of variability, one of the most noticeable characteristics of the damage track directions is their high degree of order. The nearly rectangular shapes found on specimen 1 (Figs. 10 and 11) and the parallelograms of specimen 4 (Fig. 12) were commonly observed over much of the specimens' surfaces.

This angular order was quantified by tallying the lengths of the tracks lying within eighteen 10° sectors from 0° ±5° to 170° ±5°, the angles being measured (to within ±2°) with respect to a reference straight edge of the sample. Tracks of each type were summed separately except those of type 3 which were not included, not being discernible with the ×20 objective used in the survey. This was repeated over fifty fields of view for each specimen, and the angular distribution was converted to a surface density by dividing by the specimen area thus explored.

The results of this survey are presented in the histograms of Figs.13 and 14 which show the high degree of order in the track directions. In Fig.14 the data have been adjusted to a common 0° reference axis in order to facilitate a direct comparison of the noteworthy features. Also included in Fig.14 and depicted by the horizontal line through the arrow labelled "arcs" is the angular range of arcs observed in Fig.1 as measured with ±3° accuracy. Further discussion of these features is reserved for a later section of the paper.

Optical Properties of Mylar

The manufacturing process of biaxially stretching and annealing the Mylar film imparts to it an optically biaxial nature[3] so that there are two directions, the optic axes, along which light travels with zero birefringence (Fig.15). The plane defined by these axes is the optical plane, normal to which is the optical normal. In the optical plane lie the acute and obtuse bisectrices which bisect the acute and obtuse angles between the optical axes. In the case of Mylar these are normal and parallel to the film plane respectively[3]. When the film is illuminated by strongly convergent light and is viewed along the acute bisectrix through crossed polarizers, with the microscope eyepiece removed, a biaxial interference pattern is observed[3,9,10]. This interference pattern reveals the intersection of the optical plane with the plane of the film, a line referred to as the optical trace. This trace is then parallel to the obtuse bisectrix. Zolg[3] reports that the optical trace lies between 30° and 150° with respect to the initial stretch direction of the film depending on the distance from the film's edge.

In this work the specimens were cleaned with acid of any residual aluminum, the optical trace and normal were located and the angles made with the previously defined 0° line for each specimen were measured to within ±5°.

For light waves propagating normal to the film surface, the optical normal and the optical trace are in the directions of the electric field vectors in the two characteristic waves which can be called "slow" and "fast" with respect to their relative phase velocities. In this paper, the "slow" and "fast" optical directions are the directions of the associated electric vectors.

The samples were viewed through crossed polarizers and were oriented to produce the maximum extinction of transmitted light. This defined but did not distinguish between the directions of the optical normal and the optical trace. Which of the two identified axes was in the direction of the faster ray was determined by bending the specimen to provide interference colour bands and by observing the shift in the bands when viewed through a material whose slow axis was known[11]. These results are shown in Figs.13 and 14 by arrows labelled F and S for fast and slow. The results from the biaxial interference determination of the optical normal and optical trace are labelled f and s respectively; these labels are ascribed simply by association with F and S.

Chemical Etching of Mylar

The macrostructure of polymer films and surfaces has been studied by a number of techniques including x-ray diffraction[12,13] and dynamic mechanical tests[14]. One simple and direct means of revealing the surface structure of polymers is through chemical etching[4,5,15] whereby the etchant preferentially attacks some surface features and not others. With this method it is important that the solvent does not introduce any artifacts characteristic of its own interaction with the polymer, such as induced crystallization. In the case of polyethylene terephthalate (i.e., Mylar) immersed in n-propylamine, these problems are absent partly because the reaction products are themselves soluble in the etchant and are thus diffused away from the site[5,15].

Baker[5] reported that uniaxially stretched Mylar film subjected to n-propylamine etching degenerates into long ribbon-like structures of micron-sized thickness oriented along the stretch direction, and that biaxially stretched film degenerates into a "brick and mortar pattern" similarly oriented. He tentatively suggested that the regions which were attacked preferentially were in a more disordered (amorphous) state than the intact regions composed of an ordered assembly of submicron-sized spheres.

The correlation between the orientations of these surface macrostructures and the discharge tracks was investigated. Small specimens were cut from each of the four samples, and were immersed in n-propylamine at room temperature for approximately 10 hours. Because the clean-up technique is of little consequence[15], the samples were simply rinsed in water and air dried. The 10 hour immersion period resulted in the etching of the irradiated areas only; the unexposed masked areas and rear surfaces were left intact providing evidence that the electron beam significantly alters the internal structure of the Mylar surface. With a 19 hour immersion, all surfaces were found to be etched with patterns similarly shaped and oriented.

In general the features delineated by etching were

rectangular plates approximately 20 by 50 microns arranged in a brick and mortar pattern as typified by Figure 16 . The longitudinal crevasses tended to be uniformly spaced and parallel over each specimen's surface. The exception was specimen 1 whose pattern for reasons unknown consisted of elements shaped more like convex lenses than rectangles. Surface irregularities, scratches and even damage tracks were found to alter the orientation of these lines over the immediately adjacent areas. Following Baker, the longitudinal axis of the rectangles is assumed to be predominantly in the initial film stretch direction.

A number of discharge damage tracks was still visible after etching. Two etch lines were found to be exactly coincident with the long, straight type 1 damage tracks, one aligned with the predominant etch line direction and the other crossing at an angle apparently unrelated to the etch line directions. Some type 4 tracks could be seen on the rectangular plates and approximately following the etch line directions (Fig.16) , while some other type 4 tracks crossed from plate to plate at seemingly unrelated angles.

For a more meaningful comparison of angles, the most frequently occurring longitudinal and transverse etch line directions over the samples' surfaces were identified (Fig.16) under ×5 objective magnification, except for specimen 1 where the transverse direction was excluded for want of well-defined transverse lines. These directions and their corresponding ranges are marked on Figs.13 and 14 as "long. etch" and "trans. etch" and are accurate to $\pm 2°$.

Discussion and Conclusions

The discharge tracks exhibit a striking tendency to follow certain preferred directions. With each specimen the angular distribution of tracks consists of a narrow, prominent peak composed primarily of long, straight and parallel tracks of type 1, a broader secondary peak and a sector in which few or no tracks were observed. This empty sector, which is of the order of 70° wide, in each case encompasses the fast optical direction, indicating that the discharges tend to avoid this direction.

Evidence also suggests that the visible arc direction is aligned with the principal damage track direction. Any disagreement may possibly be due to the fact that the arc directions are averaged over a meter-diameter region while the damage tracks are studied on 17 mm^2 of the specimens. Equally strong evidence suggests that the visible arc direction is associated with the slow optical axis. However one can only conclude that a large fraction of the damage tracks align with the slow optical axis to within approximately $\pm 30°$ which is 3 times greater than the measurement uncertainties involved.

In all four specimens a predominant track direction lies within 30° of the longitudinal etch direction, and where the measurement was possible the transverse etch direction was aligned with a secondary track direction.

The few specimens studied indicate a tendency for the damage tracks to align with the chemical etch axes and the slow optical axis, and also a tendency for them to avoid the fast optical axis. The spread of the damage track directions may result from the discharges interacting with both the etch axes and the optical axes at the same time. The fact that the longitudinal etch axis (parallel to the initial stretch direction) was not aligned with either the fast or slow optical axes (perpendicular and parallel to the optical trace) is no cause for concern; rather this is in complete agreement with the results reported by Zolg[3], that the optical trace (parallel to the slow axis) never lies within 30° of the initial stretch direction.

References

1. L. Inge and A. Walther, "Elektrische Entladungen in Kristallen", Z. Phys., Vol. 64, No.12, pp.830-844, Sept. 1930.

2. J.A. Brydson, Plastic Materials, London, The Butterworth Group, 1975, pp.588.

3. R.W. Zolg, "The Relationship of Birefringence to the Anisotropic Physical Characteristics of Polyethylene Terephthalate Film", Polymer Engg. and Sci., Vol. 7, No.3, pp.194-197, July 1967.

4. G.C. Adams, "Structure Studies of Chemically Etched Poly (Ethylene Terephthalate) Film", Polymer Engg. and Sci., Vol. 16, No.3, pp.222-226, March 1976.

5. W.P. Baker, Jr., "Etching of Polyethylene Terephthalate", J. Polymer Sci., Vol. 57, No.165, pp.993-1007, March 1962.

6. K.G. Balmain and G.R. Dubois, "Surface Discharges on Teflon, Mylar and Kapton", IEEE Trans. Nucl. Sci., Vol. NS-26, No.6, pp.5146-5151, Dec. 1979.

7. K.G. Balmain, "Surface Discharge Arc Propagation and Damage on Spacecraft Dielectrics", Proc. ESA Symp. on Spacecraft Materials, ESA SP-145, pp.209-215, Dec. 1979.

8. E.J. Yadlowsky, R.C. Hazelton, and R.J. Churchill, "Characteristics of Edge Breakdowns on Teflon Samples", IEEE Trans. Nucl. Sci., Vol. NS-27, No.6, pp.1765-1769, Dec. 1980.

9. E.A. Wood, Crystals and Light, 2nd Ed., New York, Dover Publications Inc., 1977, Ch. 13.

10. M. Born and E. Wolf, Principles of Optics, 2nd Ed., Oxford, Pergamon Press, 1964, p.702.

11. E.A. Wood, Ibid., Ch. 11.

12. C.J. Heffelfinger and R.L. Burton, "X-Ray Determination of the Crystallite Orientation Distribution of Polyethylene Terephthalate Films", J. Polym. Sci., Vol. 47, p.289, 1960.

13. C.J. Heffelfinger and E. Lippert, Jr., "X-Ray Low-Angle Scattering from Oriented Poly(ethylene Terephthalate) Films", J. Appl. Polym. Sci., Vol. 15, pp.2699-2731, 1971.

14. R.E. Mehta and J.P. Bell, "Chain - Folding Measurements in Annealed Poly(ethylene Terephthalate)", J. Polym. Sci., Polymer Phys. Ed., Vol. 11, pp.1793-1801, 1973.

15. C.-M. Chu and G.L. Wilkes, "Superstructure in Chemically Etched Poly(ethylene Terephthalate)", J. Macromol. Sci. - Phys., Vol. B10, No.4, pp.551-578, 1974.

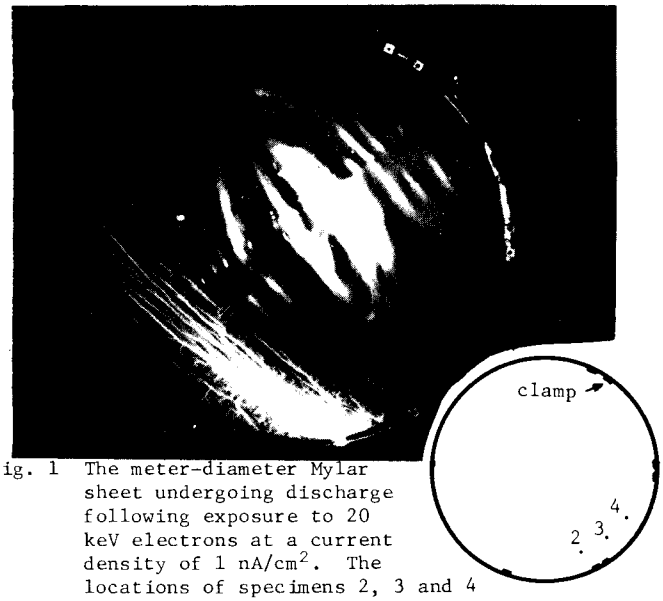

Fig. 1 The meter-diameter Mylar sheet undergoing discharge following exposure to 20 keV electrons at a current density of 1 nA/cm^2. The locations of specimens 2, 3 and 4 are indicated in the inset.

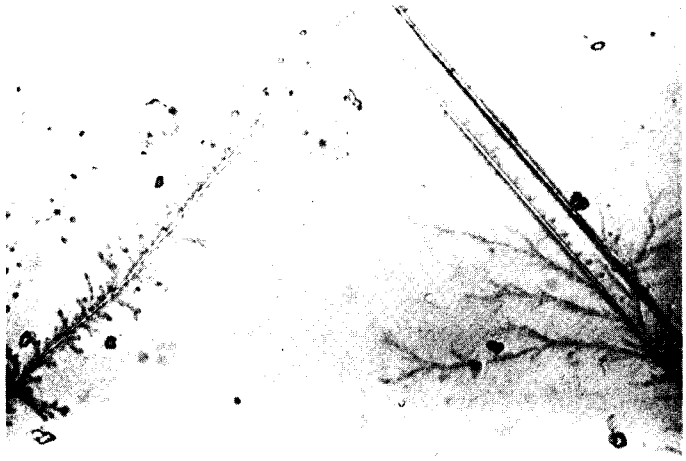

Fig. 2 Optical microscope (OM) photograph of specimen 2 under reflected light. All four track types are shown. See text for discussion. Scale: 10 μm.

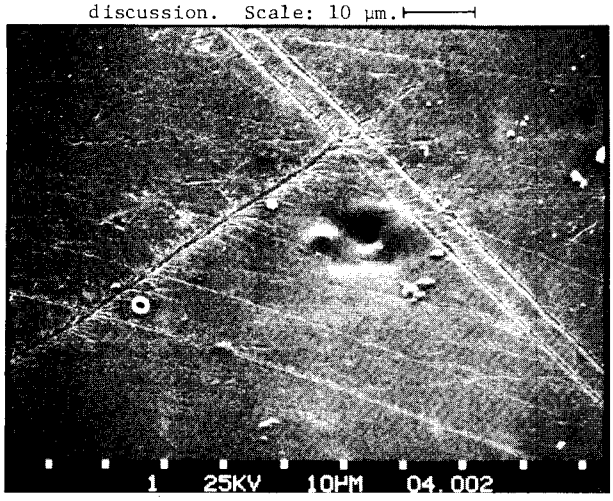

Fig. 3 Scanning electron microscope (SEM) photograph of the same feature shown in Fig.2. The faintly visible rectangles result from previous viewing at two higher magnifications. The scale shown is 10 μm per division.

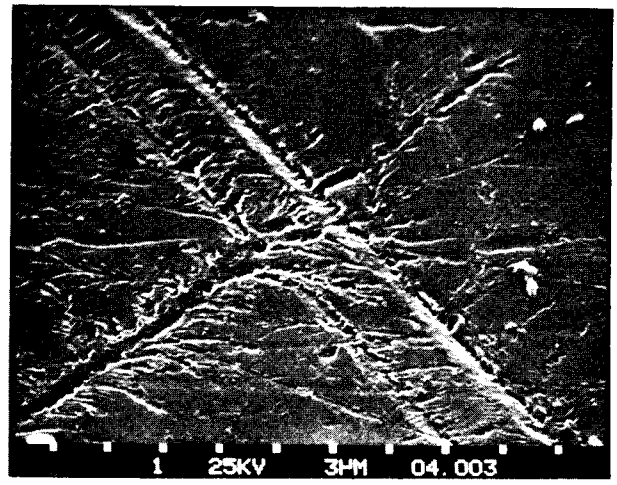

Fig. 4 Close-up of the vertex in Figs.2 and 3. Note pits comprising straight track.

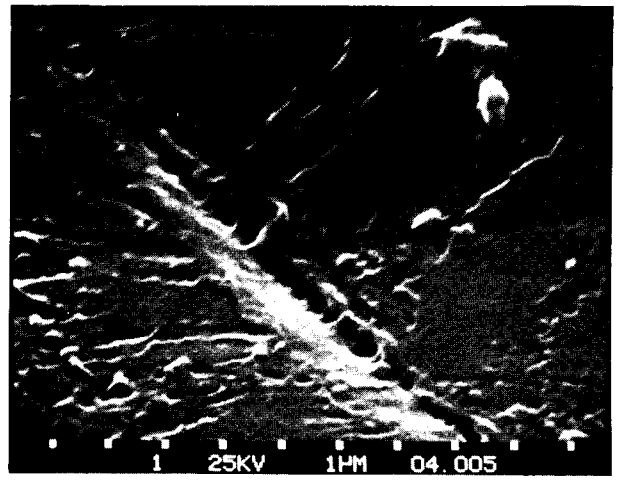

Fig. 5 Close-up of pits from lower right of Fig.4.

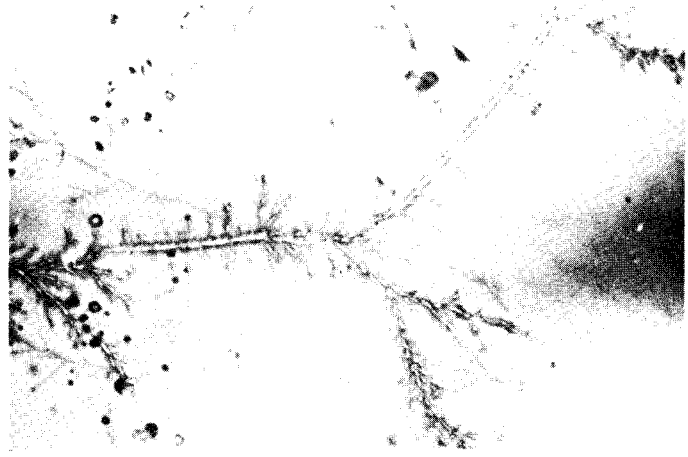

Fig. 6 Same as Fig.2 for nearby region on specimen, but only three track types shown (OM). Scale: 10 μm.

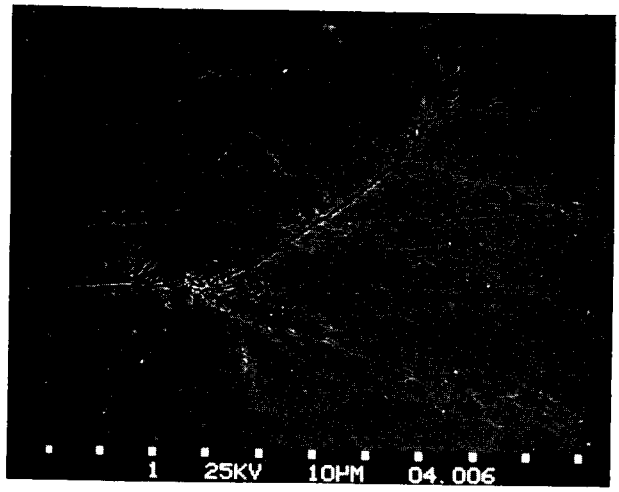

Fig. 7 SEM photograph of feature in Fig.6.

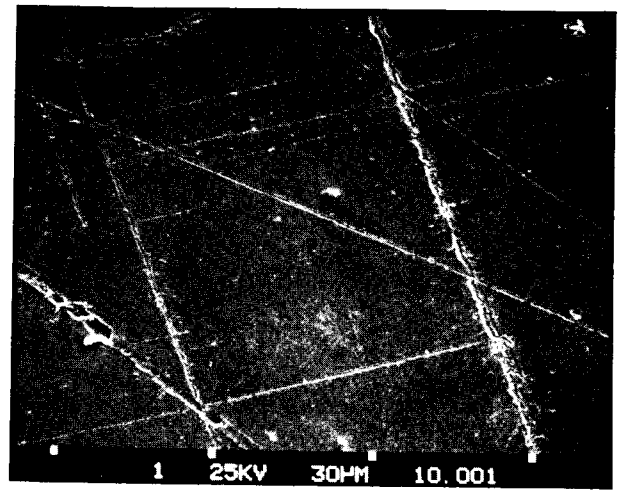

Fig.10 Regularity of damage tracks on specimen 1 (SEM).

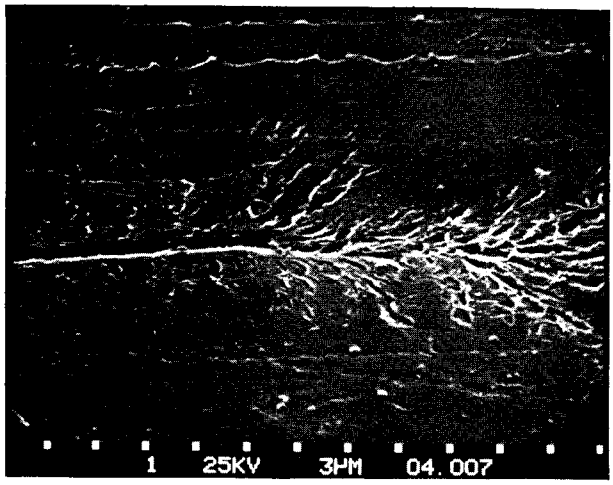

Fig. 8 Close-up of Fig.7 (SEM).

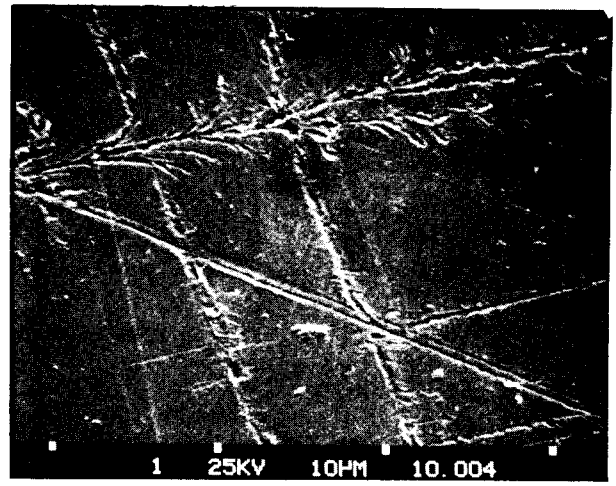

Fig.11 Close-up of upper left of Fig.10 (SEM).

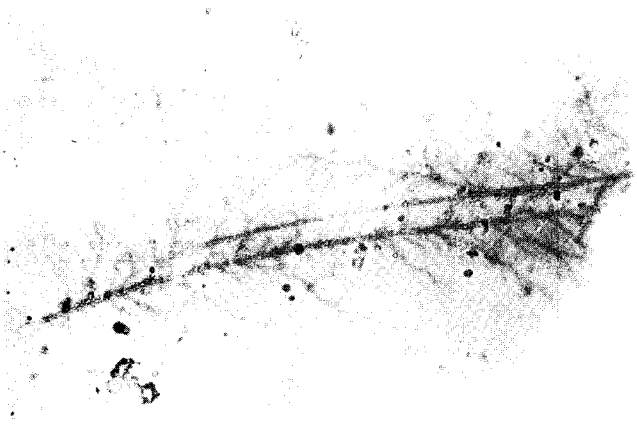

Fig. 9 Two opposing tracks of type 4 (OM). Scale: 10 µm.

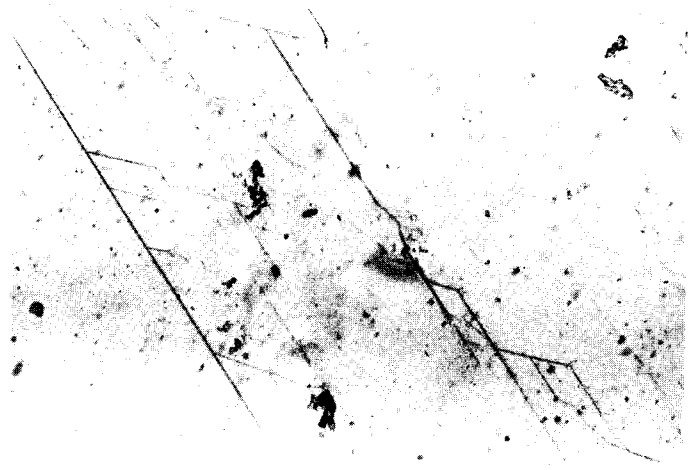

Fig.12 Regularity of damage tracks on specimen 4 (OM). Scale: 50 µm.

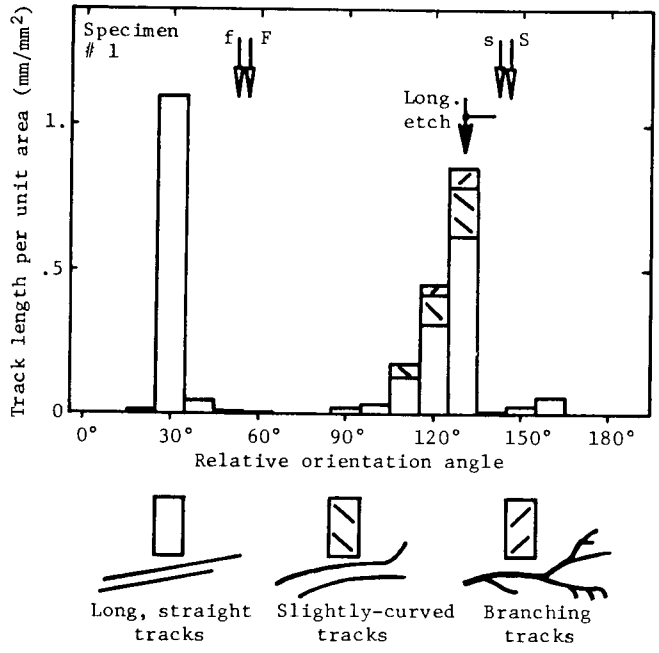

Fig.13 Discharge damage track angular distribution for 75 μm 30 cm^2 Mylar, compared with optical directions and etch-mark directions. Symbols:

F - fast optical direction.

S - slow optical direction.

f - direction of trace of optical plane.

s - direction of optical normal.

Long. etch - direction of most frequently occurring longitudinal etch lines.

Trans.etch - direction of most frequently occurring transverse etch lines.

Arcs - long arc orientations from photos.

(Note: the latter two items apply only to the following figure).

Horizontal bars attached to arrows give ranges of all associated measurements.

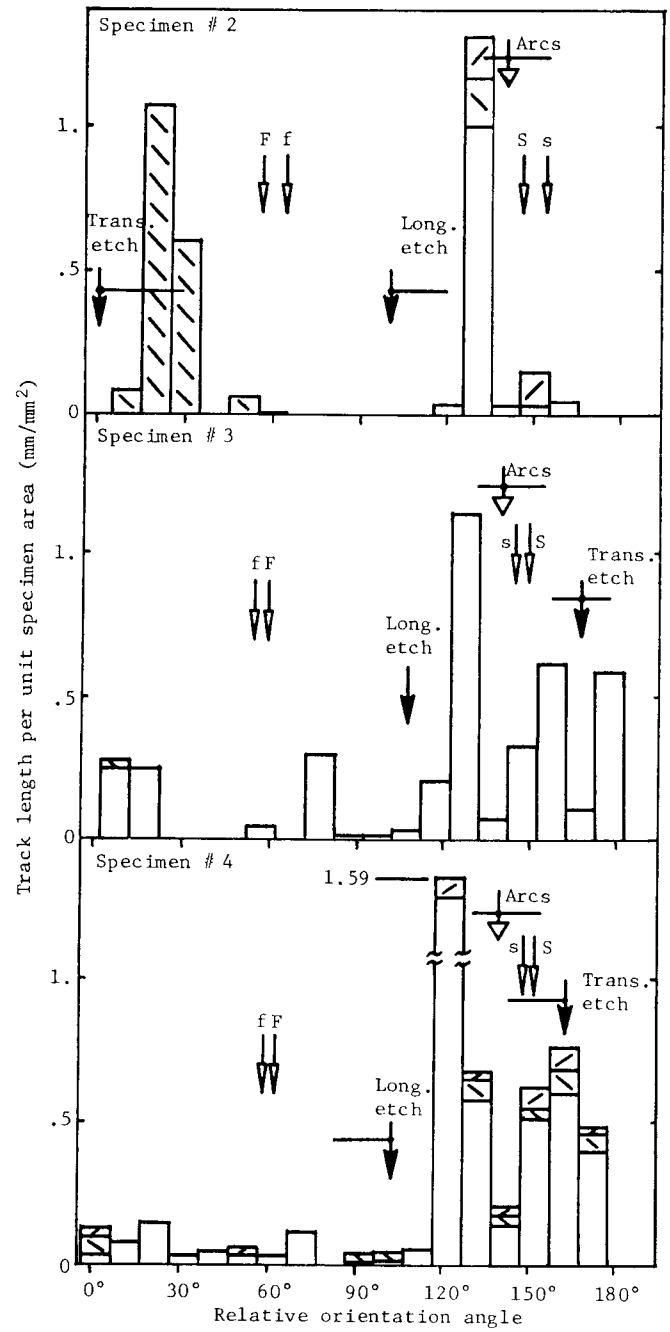

Fig.14 Same as Fig.13, but for meter-diameter Mylar.

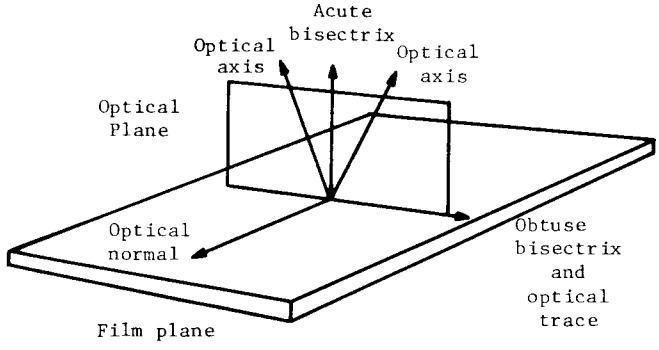

Fig.15 The characteristic directions of a biaxial, birefringent film.

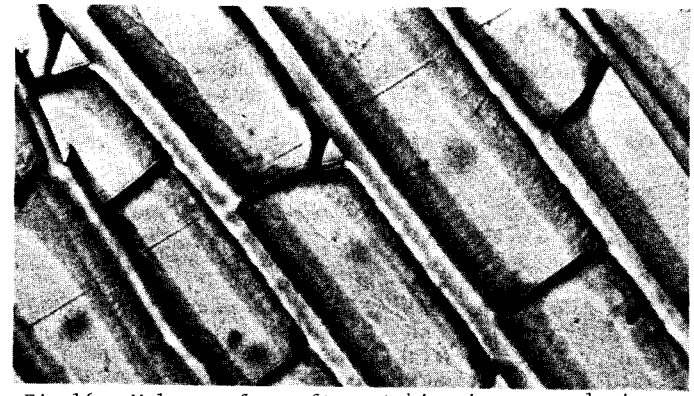

Fig.16 Mylar surface after etching in n-propylamine (OM). Note type 4 track running along central plates. Scale: 10 μm.